J.Natn.Sci.Foundation Sri Lanka 2023 51 (1): 129 - 148
DOI: http://dx.doi.org/10.4038/jnsfsr.v51i1.10785

RESEARCH ARTICLE

Geotechnical Engineering

Estimation of soil liquefaction potential in Colombo Port City (Sri Lanka) using several design earthquakes

IACC Ilangakoon* and AMRG Athapaththu
Department of Civil Engineering, Faculty of Engineering, University of Peradeniya, Peradeniya, Sri Lanka.

Submitted: 10 November 2021; Revised: 23 September 2022; Accepted: 28 October 2022

Abstract: Considering the limited land area in the Colombo Business District, the development of reclaimed land in the Colombo coastline was initiated. Colombo Port City is the first-ever mega-reclaimed land project in Sri Lanka. Land reclamations in coastal areas very often have liquefaction-related issues. Liquefaction is a process which occurs mainly due to natural seismic events. Even though Sri Lanka is located in an earthquake-free geological region, events like the 2004 Tsunami and recent studies confirmed that seismic events cannot be ignored and should be considered in the design stages of structures. Therefore, the determination of the effects of seismic events on the port city project is of prime importance. The primary purpose of this paper is to present the assessment of liquefaction triggering potential and the post-liquefaction vertical settlement. Seismic soil liquefaction was evaluated for the port city in terms of the Factor of Safety against liquefaction along with the depth of the soil profiles under the seismic demand of five earthquake scenarios that could be anticipated. The analysis process was done for 142 locations using a Cone Penetration Test-based simplified empirical procedure. The results showed that the Factor of Safety against liquefaction resistance decreases with the depth, and post-liquefaction vertical settlement is considerably high in Phase 2 land plots at the site. An earthquake with a magnitude of 6.0 and a peak ground acceleration of 0.2 has been identified as the most critical combination among the selected design seismic scenarios.

Keywords: Colombo Port City, cone penetration test, earthquake, liquefaction, simplified empirical procedure.

INTRODUCTION

Liquefaction can be identified as a serious issue in coastal reclamation projects during the event of an earthquake. The most common reason for liquefaction is natural seismic events. During an event of a natural earthquake, rapid loading is generated on saturated soil layers. Due to this rapid loading, the granular structure of the soil is distorted and causes loosely packed particle groups to collapse. Because of these collapsing mechanisms and due to the insufficient time for dissipation of excess pore-water pressure through natural drainage, a liquefaction incident occurs. Due to that, the soil no longer acts as inactive grid particles, and owing to this, the strength, stiffness, and volume of the soil particles in the liquefied areas significantly decrease. During an event of liquefaction, various types of ground failure can occur. These include loss of bearing strength, lateral spreading, vertical settlement, and flow failure.

There are some spectacular examples of liquefaction failures during earthquakes. The Niigata earthquake (Seed & Idriss, 1967), which occurred in old, reclaimed land in Japan with a magnitude of either 7.5 or 7.6, is one of the worst incidents. It took the attention of the science world, and researchers started investigations right after that event. The Hyogoken-Nambu earthquake in 1995 (Tokimatsu & Asaka, 1998), the great east Japan earthquake in the year

* Corresponding author (charith.ilangakoon@gmail.com; https://orcid.org/0009-0008-4264-4775)

of 2011 (Yasuda *et al*., 2012), and the series of earthquakes faced by New Zealand between 2010 and 2011 (Cubrinovski *et al.*, 2010) can be named major liquefaction incidents in history. The important factor is that all these mentioned failures were recorded due to the cyclic softening liquefaction.

There are several methods to evaluate the liquefaction potential. To represent the results obtained through those methods, four different main criteria can be named. Those are, in terms of a Factor of Safety (FOS), in terms of probability, in terms of liquefaction potential index (LPI) value, and in terms of the liquefaction-induced settlement. In this study, liquefaction potential was evaluated using the Factor of Safety method.

Evaluation of liquefaction potential in terms of factor of safety (FOS) is the most common approach, which is practised around the world. To calculate the FOS, various methodologies have been developed by scientists around the world. The two most commonly applied methods for the evaluation of factors of safety are the use of empirical correlations and the 'Simplified Procedure', which was proposed by Seed and Idriss (1971).

The theory behind the application of empirical correlation is based on the comparison of the grain size distribution (or any other *in situ* characteristic) of the site to the grain size envelope of sites that have liquefied in the past. When the grain size distribution of the target site falls within the envelope of grain sizes that have liquefied in history, then there is a chance of triggering liquefaction occurring at the targeted site (Shibata & Teparaska, 1988)**.**

A simply applicable empirical method was proposed by Iwasaki *et al*. (1981). It is based on the standard penetration test. The factor of safety of a specific layer can be calculated by a very simple equation (R/L) which consists only of *in situ* resistance (R) and the dynamic load induced in the soil element by a seismic motion (L). Lately, a lab-based method was presented by Hakam (2016). Inside a laboratory, artificial vibration, which is similar to an earthquake, is produced by a shaking table while measuring the acceleration and the settlement. Then by using those results, the relationship between grain size particles and the relative density associated with liquefaction resistance was determined for certain accelerations.

This study is based on the most convenient method, which is known as the simplified procedure developed by Seed and Idriss (1971). They considered a soil column as a rigid body, which is excited by the seismic loading at the base, and the shear wave propagates to the ground surface. Then the shear stress generated in the soil column was calculated by using the empirical equations proposed. The soil liquefaction mainly depends on the magnitude of the earthquake, intensity and duration of the ground motion, ground acceleration, density and effective confining pressure of the soil, thickness of the soil layer, fine content, the position of the groundwater table, and reduction of effective stress (Youd & Perkins, 1978). All these parameters can be reduced into two factors, namely, the intensity of seismic loading (cyclic stress ratio) that the soil will be subjecting to, and characterization of the liquefaction resistance (cyclic resistance ratio) of the soil. by comparing cyclic stress ratio (CSR) and cyclic resistance ratio (CRR) with each other, it is possible to quantify the value of the occurrence of liquefaction at any particular depth at a site.

The general classification is that when FOS > 1, the ground is safe, and when FOS < 1, liquefaction is said to occur (Seed & Idriss, 1971). But in reality, the soil layer can be liquefied during an earthquake, even if the FOS is more than one (Juang & Jiang, 2000). As a solution, different studies introduced higher values for the FOS against liquefaction. Sonmez (2003) advised taking into account an FOS value of 1.2 at a specific depth for the layer to be deemed safe against liquefaction. Seed and Idriss (1971) considered soil layers with an FOS value within the range of 1.25 to 1.5 as non-liquefiable. Also, Ulusay and Kuru (2004) defined soil layers with an FOS value greater than 1.2 as non-liquefiable and soil layers with an FOS of 1.0 to 1.2 as marginally liquefiable. When comparing the past studies, 1.2 can be identified as a reasonable value for FOS against liquefaction failure (Sonmez, 2003).

Preliminary estimation of liquefaction-induced ground settlement is one of the best ways to visually represent the pre-assumed liquefaction damage to a liquefaction-prone site. For level ground conditions such as Colombo port city, the amount of settlement during earthquake shaking can be computed from the volumetric re-consolidation

strains induced as the excess pore water pressure dissipate. Based on the field experience during past earthquakes, Ishihara and Yoshimine (1992) identified that the amount of volumetric strain depends on penetration resistance and the CSR applied by the designed earthquake. Based on that, authors have established a family of curves by correlating relative density (Dr) and the conventional use of FOS against liquefaction with the volumetric strain resulting from the dissipation of pore-water pressures.

Many research studies have already been carried out related to the liquefaction potential of sea sand-filled land areas around the world. But this is the very first-ever mega land reclamation project in Sri Lanka. Therefore, a comprehensive study on liquefaction potential is required to identify possible hazards related to this project, as well as for future projects of a similar nature. In this part of the world, earthquakes or seismic waves are not a common event that happens regularly. Even though there are some methodologies available for monitoring seismic events of the countries located on tectonic plate boundaries, predicting earthquakes in the middle of the tectonic plates is almost impossible. As historical data or related evidence on liquefaction are rare on the island, this study was carried out to find the liquefaction potential in Colombo port city.

The main aim of this study is to find the liquefaction potential of Colombo port city by using a CPT-based simplified liquefaction assessment method for free-field level ground conditions. The key objectives achieved in the fulfilment of the aim can be set as the analysis of liquefaction triggering potential to find the liquefaction FOS variation with depth and to estimate the post-liquefaction vertical settlement to predict the potential of liquefaction to cause damage at the surface level of the Colombo port city. Five different and anticipatable earthquake magnitudes (M) were selected for the analysis process by considering the seismicity around the island. Key results are presented in the form of the FOS contours at several depths below the ground surface, along with the spatial distribution contours for post-liquefaction settlements at the ground surface.

This study was limited to studying only the geotechnical investigation data obtained through the cone penetration tests. Since only a section of the ground area of the Phase 02 land plots was improved as the first construction phase, the availability of the cone penetration test (CPT) results for those land plots is very low. Hence an assumption was made that the liquefaction behaviour of A-7, A2-3, and A2-2 land plots is unique to the available CPT locations of the respective land plots since ground improvement for those areas has not been carried out.

The study area

Colombo port city is the first and only mega coastal reclamation project in Sri Lanka to date. This project facilitates various purposes such as commercial, residential, hospitality and recreational. The reclaimed land of the Colombo port city is divided into two main construction phases based on the structures built in the area. Most of the high-rise buildings are planned to be constructed in Phase 1 land areas, and open spaces (parks and squares, waterfronts, and beach areas) with low-rise residential buildings in Phase 2 land areas. As the first construction phase of the project, construction activities will be initiated in the Phase 1 land plots. According to the master plan, construction work in Phase 2 will be commenced after a decade. Due to that, the entire Phase 1 and only a section of Phase 2 have been treated by using different improvement methods, and the rest of Phase 2 has not been improved since there is a possibility of natural compaction in those ground areas with time. Those two phases are further divided into 14 land plots based on the land requirement. Most of the CPT boreholes are densely clustered in the areas that will be used for the construction of high-rise buildings and roads. The records from CPT tests have been collected for 142 representative borehole locations in the Colombo port city to evaluate liquefaction potential. The depths of the CPT boreholes are in the range of 8 m to 23 m. Figure 1 shows an aerial view of Colombo port city, highlighting details of CPT locations and main construction phases.

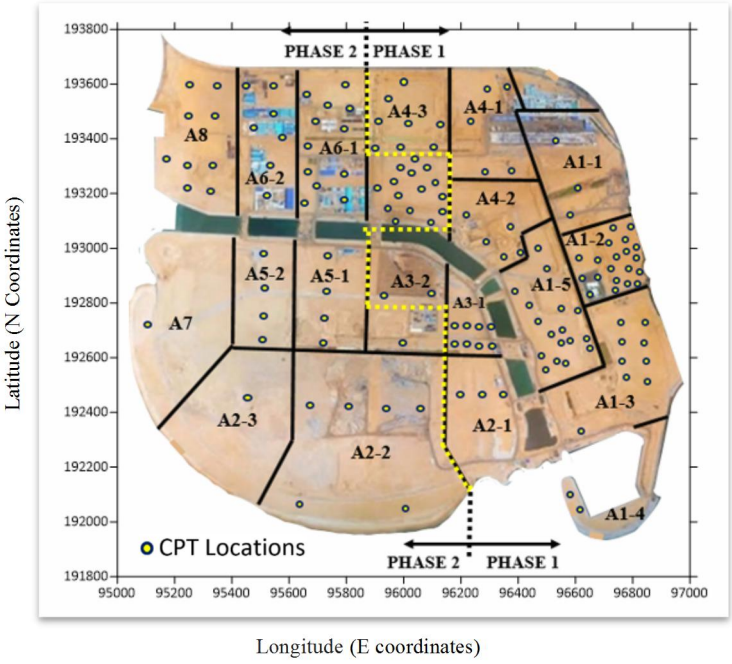

Figure 1: Aerial view of Colombo port city showing reclamation land plots, main construction phases, and locations of the 142 CPTs selected.

Earthquake ground motions

Sri Lanka lies away from the tectonic plate boundaries and the northwestern region of the Indo-Australian plate, which is known as a seismically inactive geological zone. Furthermore, intraplate seismic activities within Sri Lanka can be considered not significant (Seneviratne *et al*., 2020). Owing to this, the effect of an earthquake is minimal and there are very few studies available related to earthquakes and seismic events around Sri Lanka. However, scientists and geologists are investigating the possibility of the emergence of a new plate boundary to the south of Sri Lanka (Dissanayake, 2005). Therefore, to select appropriate earthquake magnitudes and peak ground accelerations (PGA) for this analysis, a few recently completed studies were considered. Seneviratne *et al*. (2020) researched the historical records of earthquakes around Sri Lanka and identified the 1615 earthquake as the most significant earthquake that cost over 2000 people their lives. The authors has analyzed over 300 incidents and concluded that the Mannar rift zone and Comorin ridge constitute the critical zone of influence in Sri Lanka, which can generate an event of 6.9 magnitudes (475 years return period) at a depth of 10 to 15 km in the western ocean of the island. This study also highlighted that seismicity around Sri Lanka no longer can be ignored. Hence for design purposes, it must be considered. Weerasinghe *et al*. (2020) identified that cities in the Western Province, like Colombo, Negombo, and Gampaha, that are commercialized cities, can be exposed to a PGA of more than 0.1 g (where g is the gravitational acceleration), and for Colombo, the PGA was calculated to be 0.13 g. The authors have estimated seismic hazards for the island by using a relationship called deterministic seismic hazard assessment (DSHA) and two design earthquake magnitudes of M = 6.0 and M = 6.9. Uduweriya *et al*. (2020) estimated PGA values respective to the probable return period for several areas of the country by following the probabilistic seismic hazard assessment (PSHA) technique. The PSHA technique involves calculating how often a suite of specified levels of ground motion will be exceeded at the site. The authors have used the PSHA technique with a logic tree approach to minimize the effects of epidemic uncertainty. The study produced PGA values of 0.025, 0.107, and 0.207 for return periods of 50, 475, and 2500 years, respectively. By using a finite difference method, another study was carried out by Dananjaya *et al.* (2020) to investigate the seismicity around Sri Lanka. In both DSHA and PSHA techniques, the variation of bedrock level was not taken into consideration. Therefore, in this study, numerical

simulation was carried out to investigate the effect of variation of the bedrock profile on the seismic wave propagation through Sri Lanka. As the input data, acceleration time histories of seven real-time earthquake records were selected from the Pacific Earthquake Engineering (PEER). Then the analyzing process was done by simulating two-dimensional bedrock responses. As a result of the study carried out by Dananjaya *et al.* (2020), a PGA of 0.083 value for the Colombo district was obtained. By considering the whole island, Abayakoon (1996) showed the expected value of maximum ground acceleration in Sri Lanka could be 0.28 g. With the historical records of earthquakes triggered in the close vicinity of Sri Lanka, the above value is quite reasonable. Also, Kumarasiri and Abayakoon (2008) carried out soil liquefaction analysis for the coastal line of Sri Lanka and identified a few liquefiable sites in the country, and developed a map based on that. For this study authors used an earthquake magnitude of 6.0 and a PGA value of 0.2 g as the seismic combination by considering the recommendations presented by Abayakoon (1996).

Considering the seismic scenarios in and around the island as discussed in the above literature, five design earthquake combinations have been chosen for the liquefaction analysis as given in Table 1. The magnitude of 6.9 at a 475-year return period at an epicentral distance of 90 km (placed along the failed Mannar rift zone and Comorin ridge) earthquake was selected as the control (critical) earthquake. For the second one, M = 6.0 earthquake was selected with an epicentral distance of 15 km to investigate the effect of an earthquake of magnitude lower than critical but generating at a distance closer than the critical earthquake. To investigate the effects of an earthquake with a higher magnitude and generating at the same epicentral distance as critical, M = 7.5 was selected as the third design earthquake. The same combination used in Kumarasiri and Abayakoon (2008) was selected as the fourth design earthquake combination. By considering the highest values with possibilities concluded in the literature, M = 6.9 and PGA = 0.2 was used as the final combination.

Table 1: Design seismic combinations used for the study

Seismic combination	Earthquake magnitude	PGA Value
1	6.0	0.132
2	6.9	0.1
3	7.5	0.1
4	6.0	0.2
5	6.9	0.2

MATERIALS AND METHODS

The procedure for calculation of the factor of safety and liquefaction induced settlement can be summarized as follows.

Only the sand layers beneath the groundwater table were considered. Since soil type is uniform throughout the Port City premises (marine dredged sand), the soil type was independent from the consideration for the calculation process. The depth of the sand layers (CPT Depth), thicknesses of the sand layers below the groundwater table, and depth from the groundwater table to the sand layer were considered for the analysis. Cone resistance value, sleeve friction value, friction ratio, and pore pressure value were recorded, and computation was done for the total overburden pressure and effective overburden pressure by using the geotechnical properties of the site. Then the evaluation of CRR was carried out.

Testing an undisturbed soil sample under idealized field conditions is the best way of determining CRR. But for granular/sandy soils, it is almost impossible to collect undisturbed samples and simulate *in situ* stress conditions in the laboratory. Therefore, field tests can be considered the most appropriate approach, especially for granular soils. A standard penetration test (SPT), cone penetration test (CPT), and shear-wave velocity are the commonly used

methods for the evaluation of the liquefaction resistance of sandy soils. But CPT is the most preferred *in situ* test to assess the liquefaction potential of sandy soils. The main reason is that the nearly continuous soil profile that is provided by CPTs can be developed as a liquefaction resistance profile.

After the establishment of the simplified liquefaction analysis approach, many methods based on CPT have been developed for evaluating soil liquefaction resistance (Seed & Alba, 1986; Shibata & Teparaska, 1988; Stark & Olson, 1995; Olsen, 1997; Robertson & Wride, 1998; Schneider & Mayne, 2000; Juang *et al*., 2003; Moss, 2006). Almost all of these methods follow the same format as in the simplified procedure, which judges whether the liquefaction of soil in a future seismic event will occur. But for calculating CRR in this study, the Robertson and Wride (1998) method (referred to herein as the Robertson method) was selected since it was recommended as a reliable and convenient method in a workshop organized by National Center for Earthquake Engineering Research (NCEER) in 1998 (Youd *et al.*, 2001). Also, to overcome the disadvantages of the other methods, the Robertson method developed an integrated approach, and for numerous studies, the Robertson method was adapted for the calculation of CRR (Juang *et al*., 2003; Kumarasiri & Abayakoon, 2008). Major steps involved in the calculation of CRR by using the Robertson Method are shown below. Important parameters in the Robertson method are the soil behaviour type index (Ic), equivalent clean sand normalized CPT penetration resistance ($Q_{c1N,cs}$), the correction factor for the grain characteristics of the soil (Kc), normalized CPT penetration resistance (Q), and the normalized friction ratio (F), and finally, the CRR profile for an earthquake of magnitude (M) equal to 7.5, denoted as $CRR_{7.5}$.

Robertson and Wride method

1. Calculation of *in situ* stresses (Total vertical stress (σ_{v0}) and effective vertical stress (σ_{v0}')).
2. Calculation of normalized cone resistance (Q) and normalized friction ratio (F).
3. Calculation of soil behavior type index (Ic).
4. Calculation of cone penetration resistance which corrected for overburden stresses (Qc1N).
5. Calculation of the correction factor (Kc) which is a function of the grain characteristics.
6. Calculation of the equivalent clean sand normalized penetration resistance [(Qc1N) cs].
7. Determination of the CRR for earthquake magnitude of M = 7.5.

After the determination of CRR, an evaluation of the cyclic stress ratio (CSR) was carried out. CSR can be determined from the peak ground acceleration (PGA) that depends upon site-specific ground motion. The equation for CSR induced by earthquake ground motions formulated by Seed and Idriss (1971) is shown in equation (1),

$$\mathrm{CSR} = 0.65 \left(\frac{\sigma_v}{\sigma_v'}\right)\left(\frac{a_{max}}{g}\right) r_d \qquad \ldots(1)$$

where,

σ_v = Total vertical stress at the depth Z
σ'_v = Effective vertical stress at the depth Z
g = Acceleration of gravity
a_{max} = Peak ground acceleration
r_d = Shear stress reduction factor for depth Z given by equation (2).

$$r_d = \begin{cases} 1.0 - 0.00765\,z, & z \le 9.15\mathrm{m} \\ 1.174 - 0.0267\,z, & 9.15 < z \le 23m \end{cases} \qquad \ldots(2)$$

In true conditions, the soil does not behave like a rigid body. Soil behaves more like a flexible body, and in the above equation (1), rigid body shear stress is reduced with a correction factor (r_d) or stress reduction factor to obtain the deformable body shear stress with depth (Seed & Idriss, 1971). The factor of 0.65 is to reduce the maximum shear stress. Therefore it is reasonably accurate to use for the calculation process. This originally developed

simplified equation can only be applied to earthquakes with a magnitude of 7.5. For different earthquake magnitudes, a factor called 'magnitude scaling factor' (MSF) should be used for the calculation process. In this research, MSF values proposed by Seed and Idriss (1982) were used for the calculation process. According to Seed and Idriss, the magnitude scaling factor is given by equation (3).

$$\mathrm{MSF} = \left(\frac{\mathrm{Mw}}{7.5}\right)^{n}; n = -2.56 \quad \ldots(3)$$

PGA is the maximum ground acceleration that occurs during earthquake shaking at a particular location. It is not measured from the total energy that dissipates during an event. It is usually calculated by considering how hard the earth is shaking at that particular event. PGA is normally considered to be fixed for a specific region.

After all inclusions of factors, the final version of CSR used in this study was derived as equation (4):

$$\mathrm{CSR} = 0.65\left(\frac{\sigma_{\mathrm{v}}}{\sigma'_{\mathrm{v}}}\right)\left(\frac{a_{max}}{\mathrm{g}}\right)\frac{r_d}{MSF} \quad \ldots(4)$$

Finally, the computation of the factor of safety for the specific layer from the simplified method as shown in equation (5).

$$\mathrm{F.O.S.} = \frac{CRR}{CSR} \quad \ldots(5)$$

The same procedure was followed for the calculation of the factor of safety at the other CPT depths of the same soil profile. Determination of post-liquefaction site settlement values by using the FOS values generated by the Robertson and Wride (1998) method was carried out as the final step of the calculation process. The procedure involved in the calculation of FOS and vertical settlement is as follows.

Calculation of factor of safety and vertical settlement

Consider a borehole log 'C-184' of the 'A4-3' land lot in Phase 01 of the Colombo Port City premises.
The selected sand layer is 17 m below the ground surface and 12.42 m below the groundwater table. The ground water table is located around 4.58 m below the ground surface.

CPT parameters at 17 m below the ground surface are,

- Cone resistance (qc) in MPa = 8.05
- Sleeve friction (fs) in MPa = 0.03
- Friction ratio (Rf) in % = 0.38

Table 2: Parameters of the selected CPT location C184

Parameter	Value
Water density (γ_w)	9.81 kN/m^3
Bulk unit weight of fill sand (γ_b)	18.00 kN/m^3
Water level (Z_w)	4.58 m
CPT level (Z)	17.00 m

1. Calculation of the in-situ stresses at 17 m below the ground surface by considering the unit weight of marine dredged sand used in the Colombo Port City as 18 kN/m³,

σ_{v0} = (Z) (γ_b)
= 17.00 x 18.00
= 306.00 kPa

σ_{v0}' = ((Z_w) (γ_b) + [(Z- Z_w) x (γ_b - γ_w)]
= 4.58 x 18.00 + [12.42 x (18-9.81)]
= 184.15 kPa

2. Evaluation of cyclic stress ratio (CSR)

a) Calculation of shear stress reduction factor (r_d) for depth Z from equation (2).

r_d = $1.174 - 0.0267z$
= 1.174 – 0.0267(17)
= 0.732

b) Estimation of peak ground acceleration (PGA).

Table 3: Seismic combinations and the PGA values

Seismic combination	PGA value
1	0.132 g
2	0.1 g
3	0.1 g
4	0.2 g
5	0.2 g

c) Calculation of MSF from equation (3).

Table 4: Seismic combinations and the MSF values.

Seismic combination	Earthquake magnitude	MSF value
1	6.0	$\left(\frac{6.0}{7.5}\right)^{-2.56} = 1.77$
2	6.9	$\left(\frac{6.9}{7.5}\right)^{-2.56} = 1.23$
3	7.5	$\left(\frac{7.5}{7.5}\right)^{-2.56} = 1.00$
4	6.0	$\left(\frac{6.0}{7.5}\right)^{-2.56} = 1.77$
5	6.9	$\left(\frac{6.9}{7.5}\right)^{-2.56} = 1.23$

d) Determination of CSR from equation (1).

Table 5: Seismic combinations and the CSR values for C184 at 17 m depth.

Seismic combination	PGA value	CSR value
1	0.132 g	$0.65\left(\frac{306}{184.15}\right)\left(\frac{0.132g}{g}\right)\frac{0.732}{1.77}$ = 0.059
2	0.1 g	$0.65\left(\frac{306}{184.15}\right)\left(\frac{0.1g}{g}\right)\frac{0.732}{1.23}$ = 0.064
3	0.1 g	$0.65\left(\frac{306}{184.15}\right)\left(\frac{0.1g}{g}\right)\frac{0.732}{1.00}$ = 0.079
4	0.2 g	$0.65\left(\frac{306}{184.15}\right)\left(\frac{0.2g}{g}\right)\frac{0.732}{1.77}$ = 0.089
5	0.2 g	$0.65\left(\frac{306}{184.15}\right)\left(\frac{0.2g}{g}\right)\frac{0.732}{1.23}$ = 0.13

3. Evaluation of cyclic resistance ratio (CRR)

Robertson and Wride (1998) method

a) Calculation of normalized cone resistance (Q) and normalized friction (F) ratio.

$Q = (qc - \sigma_{v0}) / \sigma_{v0}'$
$= (8.05 - 0.306) / 0.184$
$= 42.08$ MPa

$F = [fs / (Qc - \sigma_{v0})] * 100\ \%$
$= [0.031/ (8.05 - 0.306)] * 100\ \%$
$= 0.4$

b) Calculation of soil behavior type index (Ic).

$Ic = [(3.47 - \log Q)^2 + (\log F + 1.22)^2]^{0.5}$
$= [(3.47 - \log 42.08)^2 + (\log 0.4 + 1.22)^2]^{0.5}$
$= 2.016$

c) Ic < 2.6, so the calculation of cone penetration resistance corrected for overburden stresses (Qc1N).

$$Qc1N = \left(\frac{Qc}{Pa2}\right)\left(\frac{pa}{\sigma v0'}\right)^{0.5}$$
$$= \left(\frac{8.05}{0.1}\right)\left(\frac{0.1}{0.184}\right)^{0.5}$$
$$= 59.34 \text{ MPa}$$

d) Calculation of corrected soil behavior type index (Ic).

$$Ic = [(3.47 - \log Qc1N)^2 + (\log F + 1.22)^2]^{0.5}$$
$$= [(3.47 - \log 59.34)^2 + (\log 0.4 + 1.22)^2]^{0.5}$$
$$= 1.88$$

e) Calculation of the correction factor (Kc) which is a function of the grain characteristics.

$1.64 < Ic < 2.36$ and $F < 0.5$ %,

Hence,

$Kc = 1$ ($1.64 < Ic < 2.36$ and $F < 0.5\%$)

f) Calculation of the equivalent clean sand normalized penetration resistance [$(Qc1N)_{cs}$].

$$(Qc1N)_{cs} = (Kc)\,(Qc1N)$$
$$= (1)\,(59.34)$$
$$= 59.34 \text{ MPa}$$

g) Determination of the CRR for earthquake magnitude of M = 7.5.

$$CRR_{7.5} = 0.833\left(\frac{(Qc1N)cs}{1000}\right) + 0.05$$
$$= 0.833\left(\frac{59.34}{1000}\right) + 0.05$$
$$= 0.1$$

4. Computation of the factor of safety for the specific layer from equation 05

Layers with FOS values of lesser than 1.2 have been considered as locations that are susceptible to liquefaction. By repeating the same procedure, FOS values for all the soil layers located below the water table can be calculated.

Table 6: Calculated FOS values for C184 at 17 m depth.

	CSR Value	Robertson Method	
Seismic Combination		CRR Value	FOS
1	0.059	0.1	1.69
2	0.064	0.1	1.56
3	0.079	0.1	1.26
4	0.089	0.1	1.12
5	0.130	0.1	0.76

5. Determination of post-liquefaction site settlement values by using the FOS values generated by the Robertson method.

This method is essentially based on estimating the maximum cyclic shear strain of each layer during and after liquefaction which is estimated from the FOS against liquefaction and Relative Density of dredged sand (Dr), Where Dr can be correlated from CPT data based on the following equation (6) proposed by Tatsuoka and Asaka (1998).

Step 01: The factor of safety against liquefaction, FOS, has to be evaluated for each layer of sand deposits at a given location by any conventional method. For this study, FOS values obtained through the Robertson method were used.

Step 02: Calculation of Relative Density (Dr) value using equation No. 06.

$$Dr = -85 + 76\log(Qc1N) \quad \ldots(6)$$
$$= -85 + 76\log(59.34)$$
$$= 49.77\ \%$$

Step 03: Calculation of maximum cyclic shear strain for post-liquefaction settlement by using the chart proposed by Zhang *et al.* (2004).

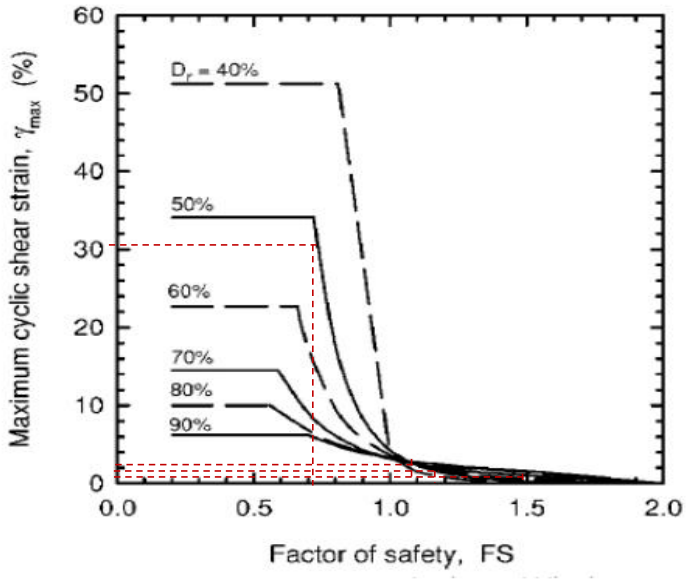

Figure 2: Maximum cyclic shear strain for post liquefaction lateral displacement proposed by Zhang *et al.* (2004).

Table 7: Calculated FOS values and maximum cyclic shear strain values for C184 at 17 m depth.

Seismic Combination	FOS Value	Maximum Cyclic Shear Strain (γ)
1	1.69	0.0
2	1.56	1.0
3	1.26	1.8
4	1.12	2.9
5	0.76	30.1

Step 04: Calculation of volumetric strain (ε) due to post-cyclic reconsolidation settlement by using the chart proposed by Ishihara and Yoshimi (1992).

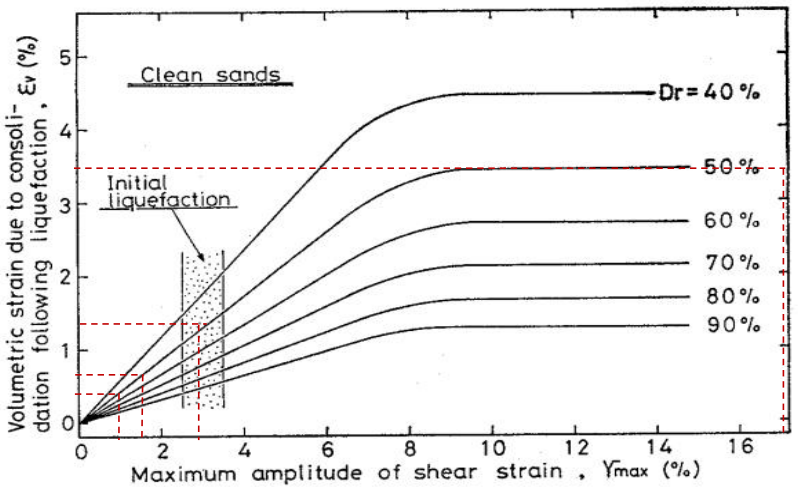

Figure 3: Recommended relationships for volumetric re-consolidation strains as a function of maximum shear strain and relative density (Ishihara & Yoshimi, 1992)

Table 8: Calculated maximum cyclic shear strain volumetric strain (γ) values and volumetric strain (ε) for C184 at 17m depth.

Seismic combination	Maximum cyclic shear strain (γ)	Volumetric strain (ε) %
1	0.0	0.00
2	1.0	0.35
3	1.8	0.70
4	2.9	1.40
5	30.1	3.30

Step 05: Settlement of the specific layer can be obtained by multiplying the volumetric Strain and the thickness of the layer as shown in equation No. 7.

Settlement = (Volumetric strain) (Layer thickness)

$$S = (\varepsilon)(\Delta Z) \quad \ldots(7)$$

Step 06: The determined volumetric strains can be multiplied by the respective layer thickness to obtain the settlement of the specific layer. Then by summing the settlement of the each layer, it is possible to determine the entire amount of ground settlement from using the equation 8.

$$S = \sum_{i=1}^{j} \varepsilon_{vi} \Delta Z_i \quad \ldots(8)$$

where,

S = Liquefaction-induced ground settlement

ε_{vi} = Post-liquefaction volumetric strain for the soil sublayer i

Δz_i = Thickness of the sublayer i

j = Number of soil sublayers.

RESULTS AND DISCUSSION

Considering the high importance of the Colombo port city, this study attempts to evaluate the FOS against liquefaction and corresponding post-liquefaction settlement for the worst seismic scenarios for the port city, using the CPT-based simplified method. To illustrate the variation of the FOS of soils with depth, the result of the analysis for a representative profile from land plot A4-3 (C-184) in Colombo port city is shown in Figure 4.

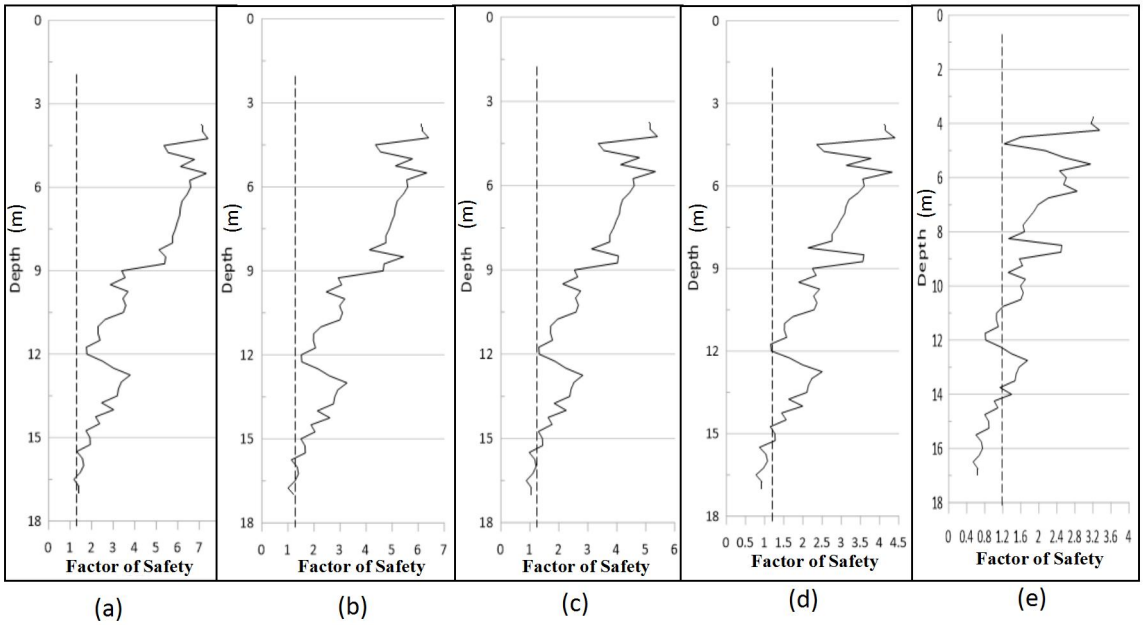

Figure 4: FOS values against liquefaction (a) combination 1; (b) combination 2; (c) combination 3; (d) combination 4; (e) combination 5.

The typical computation of FOS against liquefaction for earthquakes of different magnitudes is carried out at this representative borehole. It could be noted that the value of FOS is decreasing along with the depth of the selected borehole. Also, it is noted that the thickness of the liquefiable layers is increasing with the higher magnitudes of earthquakes.

Analysis was carried out by assuming five earthquake combinations, which may feasibly be triggered in and around Sri Lanka. Among the analyzed locations, some land plots in the Phase 02 section of the Colombo port city premises were found to be susceptible to soil liquefaction as per the simplified procedure.

The contour maps for the factor of safety values at 6 m, 12 m, and 18 m depths were mapped for the generation of liquefaction-susceptible zones. A remarkable reduction in the factor of safety values along the depth of the profiles was identified for almost all locations.

Figures 5 to 9 present the spatial distribution of the factor of safety values against liquefaction at 6.0 m, 12.0 m, and 17.0 m depths for five selected seismic combinations, respectively. It can be noted that the FOS values at a depth of 6 m are much higher than the values at 12 m and 17 m depths for all five earthquakes. Spatial distribution values for 17 m depth are pretty much similar to the 12 m depth values. But only for some locations, the value for 17 m depth is slightly lesser than that for 12 m depth.

It is obvious from the Figures 5 to 9 that the design earthquake combinations with M = 6.9 and PGA = 0.2 and, M = 6.0 and PGA = 0.2 have the lowest range of FOS spatial distribution values for all three depth ranges. The highest FOS values were recorded against M = 6 and PGA = 0.132 design earthquake. Values plotted for control earthquakes (M = 6.9 and PGA = 0.1) and earthquakes with a magnitude of 7.5 are varying within the same limits. From the contours of the FOS shown below, it is evident that for most of the locations, FOS values at all depths are higher than the established safe value of 1.2.

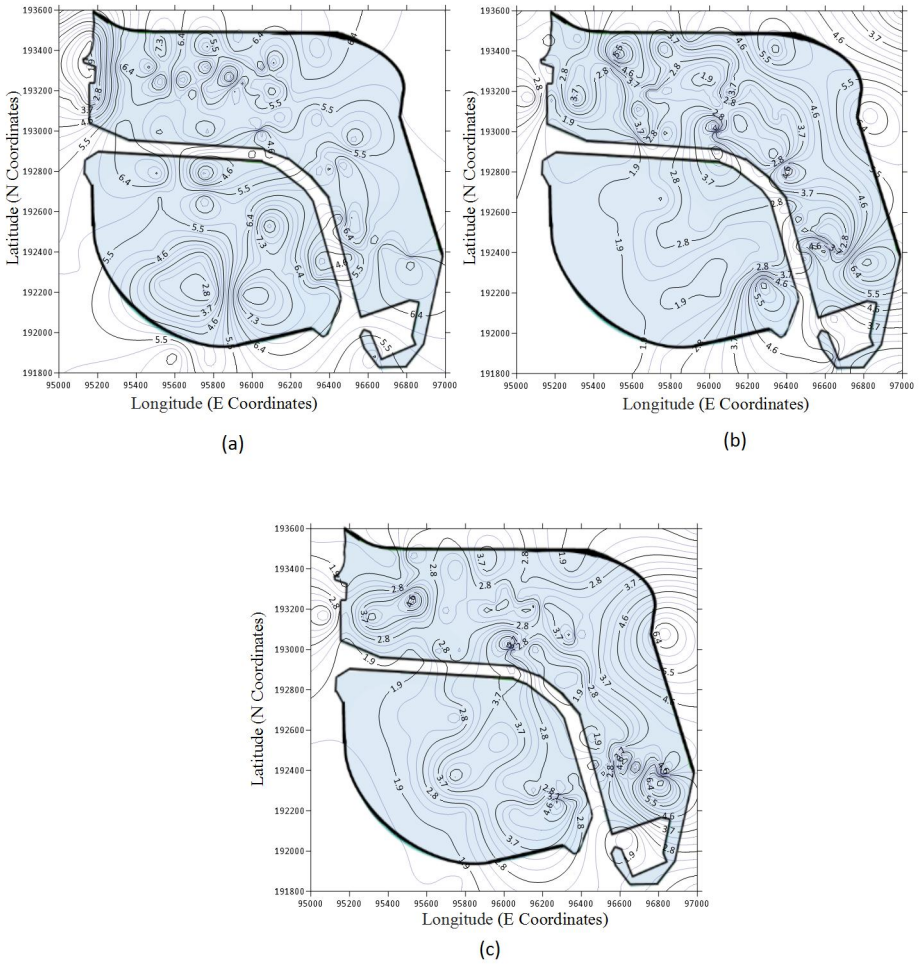

Figure 5: Contours of FOS against liquefaction potential for combination 1, (a) at a depth of 6 m; (b) at a depth of 12 m; (c) at a depth of 17 m, from the Robertson method.

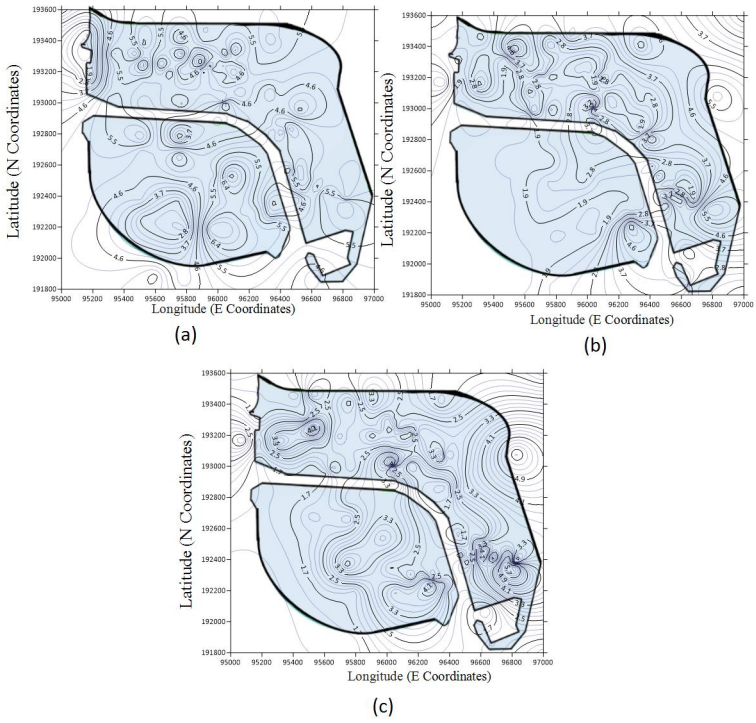

Figure 6: Contours of FOS against liquefaction potential for combination 2, (a) at a depth of 6 m; (b) at a depth of 12 m; (c) at a depth of 17 m, from the Robertson method.

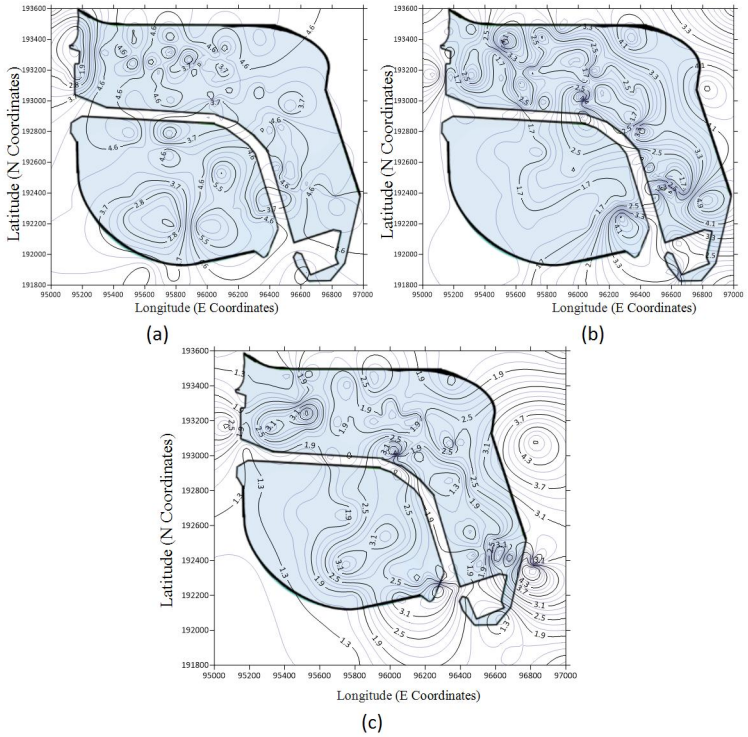

Figure 7: Contours of FOS against liquefaction potential for combination 3, (a) at a depth of 6 m; (b) at a depth of 12 m; (c) at a depth of 17 m, from the Robertson method.

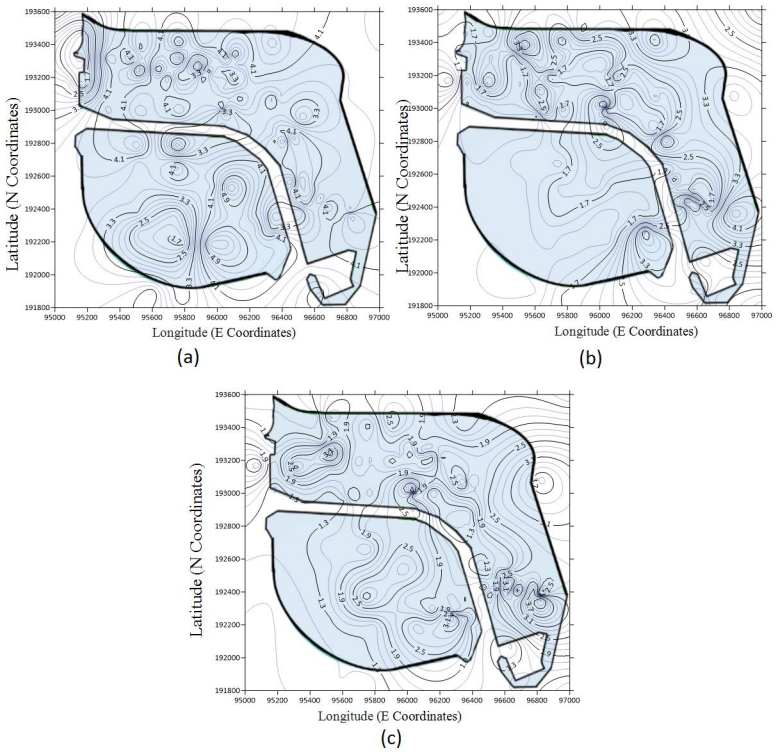

Figure 8: Contours of FOS against liquefaction potential for combination 4, (a) at a depth of 6 m; (b) at a depth of 12 m; (c) at a depth of 17 m, from the Robertson method.

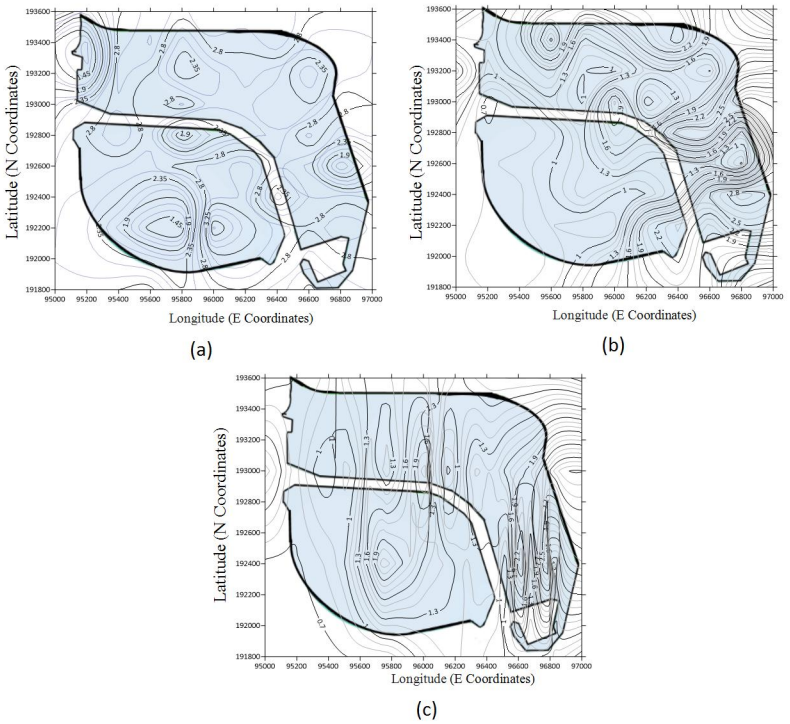

Figure 9: Contours of FOS against liquefaction potential for combination 5, (a) at a depth of 6 m; (b) at a depth of 12 m; (c) at a depth of 17 m, from the Robertson method.

These contours show the liquefaction vulnerability at different sites in the city. Liquefaction susceptibility for sites with FOS less than 1.2 can be identified as very high. Some of the land plots in the city, namely A8, A6-2, A6-1, A5-2, and A5-1 are highly vulnerable to severe liquefaction for earthquake combinations of 3, 4, and 5, according to the results generated.

To get a visual representation of analyzed boreholes, the results of the liquefaction triggering assessment of all 142 locations at the reclamation zone, under the control earthquake with seismic demand of the Mw = 6.9 and PGA = 0.1, are shown in Fig. 10 (a) in terms of the CSR (normalized for M = 6.9 and σ'_v = 100 kPa, denoted as $CSR_{6.9}$) as a function of the clean sand-equivalent corrected cone tip resistance (Q_{c1Ncs}).

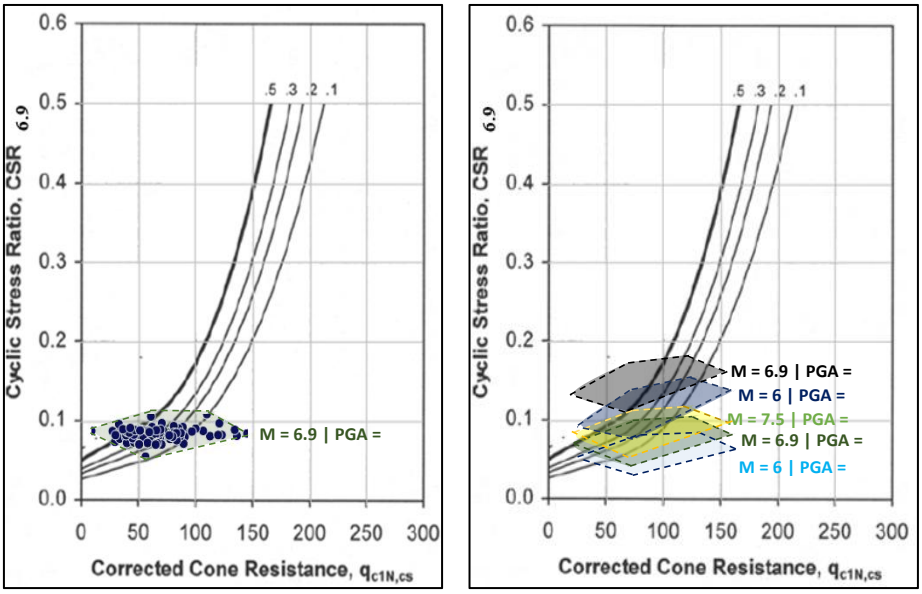

Figure 10: (a) Results of the simplified triggering analysis for CPT profiles for the control earthquake; (b) results of the simplified liquefaction triggering analysis for CPT profiles for the design earthquake combination 1, 3, 4 and 5 shown as general ranges of median CSR and Q_{c1Ncs} at each profile.

Each point represents the median Qc1Ncs and CSR value in the critical layer for a single CPT location. CRR curves for the Probability of Liquefaction (PL) of 10%, 20%, 30%, and 40% given in the Robertson method are also plotted in the same graph for reference. It was noted that against the control earthquake of M = 6.9 and PGA = 0.107, most of the critical layers were plotted within the probability range of 30% to 50% and a few above the 50% line. Liquefaction triggering assessment under the seismic demands of the M = 6.0 / PGA = 0.132, M = 7.5 / PGA = 0.1, M = 6.0 / PGA = 0.2, and M = 6.9 / PGA = 0.2 earthquakes were also performed for the critical layers of all 142 CPT locations considered, and values are shown as box plots in Figure 10 (b), as general ranges of median CSR and Qc1Ncs, concerning the control earthquake values. Results from this liquefaction triggering analysis show that all of the considered CPT locations can be identified as safe against the Mw = 6.0 / PGA = 0.132 earthquakes since respective CSR values, as plotted, appear below the 50% triggering curve. The earthquake combination with Mw = 7.5 and PGA = 0.1 has the same distribution of the results as the control earthquakes, with marginally higher CSR values. Against the earthquakes with Mw = 6.0 / PGA = 0.2 and Mw = 6.9 / PGA = 0.2, the most critical layers of

CPT profiles were plotted to appear above the 50% triggering curve. Hence special attention should be drawn to those locations with higher liquefaction triggering potential, which exceeds 50% against all four design earthquakes.

Figure 11 illustrates the spatial distribution of the estimated liquefaction-induced ground settlements for the Colombo port city, which was developed to predict the damage of liquefaction-induced settlement against the design earthquake combinations of magnitude Mw = 6.9 / PGA = 0.1, Mw = 7.5 / PGA = 0.1, Mw = 6.0 / PGA = 0.2 and, Mw = 6.9 / PGA = 0.2.

It was noted that vertical settlement against the earthquake combination 1, Mw = 6.0 / PGA = 0.132 is almost negligible, and the highest settlement values were estimated against the earthquake combination with Mw = 6.9 / PGA = 0.2, which was recorded around 600 mm (Figure 11) at Land Plot 8 which is located in Phase 2. Against the Mw = 6.0 / PGA = 0.2 and Mw = 7.5 / PGA = 0.1 earthquakes, post-liquefaction induced settlements were calculated as much higher compared to the control earthquake of Mw = 6.9 / PGA = 0.1. Also, the settlement values in Phase 2 land plots increase considerably with an increase in the magnitude of the earthquake.

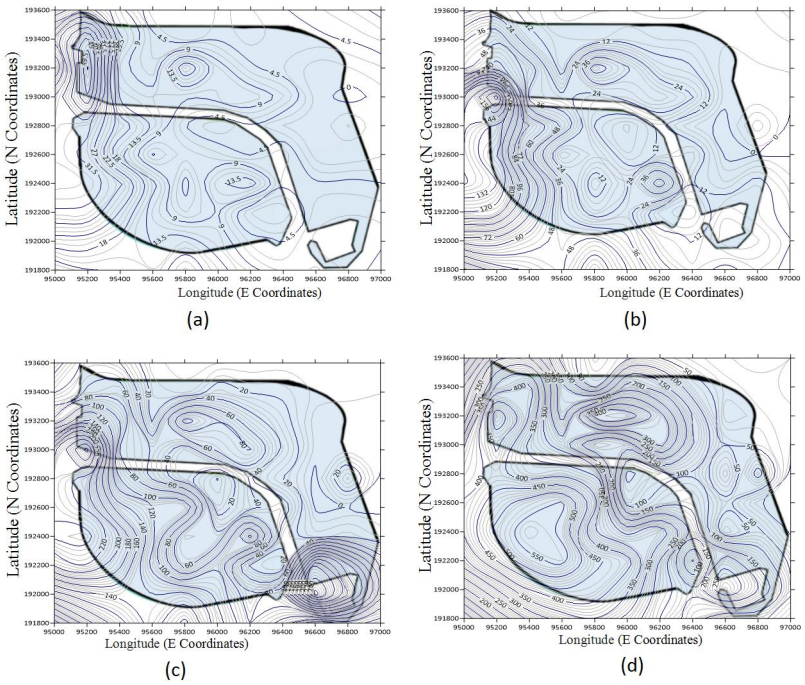

Figure 11: Contours of liquefaction-induced settlement values, (a) combination 2; (b) combination 3; (c) combination 4; (d) combination 5.

CONCLUSION

Under the present study, deterministic liquefaction triggering analysis was assessed by employing the CPT-based simplified method for free-field level ground conditions along with the post-liquefaction vertical settlement analysis.

The results revealed that the FOS values decrease along the depth under the seismic demand of considered design earthquakes. The effective depth of ground improvement, being only 6 m could be the reason for this observation. However, it is noted that critical layers in some CPT locations have a high possibility of liquefaction triggering with more than a 50% probability value. The probability of liquefaction triggering and liquefaction-induced ground settlement was considerably high in the Phase 2 ground plots, where limited improvements were carried out. Also, the maximum spatial distribution of settlements was calculated against the design earthquake

combinations with M = 6.9 / PGA = 0.2 and M = 6.0 / PGA = 0.2. According to the assumptions made due to the unavailability of CPT data in unimproved areas in Phase 2, it can be concluded that the actual FOS and settlement values are less than the values obtained from the contours since those values are based on available CPTs located in improved land areas in Phase 2.

Furthermore, out of five seismic design combinations, M = 6.9 / PGA = 0.2 and M = 6.0 / PGA = 0.2 have been identified as the most critical combinations in terms of post-liquefaction induced settlement and liquefaction triggering locations. Therefore, both earthquake combinations with M = 6.9 / PGA = 0.2 and M = 6.0 / PGA = 0.2 can be used for future assessment work and design work of Colombo port city or any other reclamation project located in Colombo.

Some of the land plots in Phase 2 of the city are highly vulnerable to severe liquefaction triggering and liquefaction-induced vertical settlement for the five earthquake combinations selected. These contour maps will help structural designers and city planners to check the vulnerability of the area against liquefaction. Also, these maps can be used effectively for future seismic safety plans and seismic hazard mitigation programs.

REFERENCES

Abayakoon S.B.S. (1996). Seismic risk analysis of Sri Lanka. *Journal of the Geological Society of Sri Lanka* **6**: 65–72.

Cubrinovski *et al.* (13 authors) (2010). Geotechnical reconnaissance of the 2010 Darfield (Canterbury) earthquake. *The Bulletin of the New Zealand Society for Earthquake Engineering* **43**(4): 243–320. DOI:https://doi.org/10.5459/bnzsee.43.4.243-320

Dissanayake C. (2005). A new plate boundary near Sri Lanka; Implications for future geo hazards. *Journal of the National Science Foundation of Sri Lanka* **33**(1): 5–8. DOI: https://doi.org/10.4038/jnsfsr.v33i1.2361

Dananjaya R.M.S., Wijesundara K.K., Seneviratne H.N. & Dissanayake P.B.R. (2020). Determination of response spectra for Sri Lankan cities using finite difference method. *Engineer* **53**(3): 45–52. DOI: https://doi.org/10.4038/engineer.v53i3.7419

Hakam A. (2016). Laboratory liquefaction test of sand based on grain size and relative density. *Journal of the Engineering Technology Science* **48**(3): 334–344. DOI: https://doi.org/10.5614/j.eng.technol.sci.2016.48.3.7

Ishihara K. & Yoshimine M. (1992). Evaluation of settlements in sand deposits following liquefaction during earthquakes. *Soils and Foundations* **32(**1): 173–188. DOI: https://doi.org/10.3208/sandf1972.32.173

Iwasaki T., Tokida K. & Tatsuoka F. (1981). Soil liquefaction potential evaluation with use of the simplified procedure. *Proceeding of the International Conference on Recent Advance in Geotechnical Earthquake Engineering and Soil Dynamics*, 28 April. Missouri University of Science and Technology, St. Louis, USA, pp. 209–214.

Juang C.H., Yuan H., Lee D.H. & Lin P.S. (2003). Simplified cone penetration test-based method for evaluating liquefaction resistance of soils. *Journal of the Geotechnical Geoenvironment Engineering* **129**(1): 66–80. DOI: https://doi.org/10.1061/(ASCE)1090-0241(2003)129:1(66)

Juang C.H & Jiang T. (2000). Assessing probabilistic methods for liquefaction potential evaluation. *Geotechnical Special Publication* **107**: 148–162. DOI: https://doi.org/10.1061/40520 (295)10

Kumarasiri H.C. & Abayakoon S.B.S. (2008). Potential of soil liquefaction in Sri Lanka- A dynamic approach to the mitigation of natural disasters. *Proceedings of Symposium of International Institute for Infrastructure Renewal and Reconstruction (IIIRR),* April 2008. University of Calgary, Canada, pp. 10–12.

Moss R.E.S. (2006). CPT-based probabilistic and deterministic assessment of in situ seismic soil liquefaction potential. *Journal of the Geotechnical Geoenvironment Engineering* **132**(8): 1032–1051. DOI: https://doi.org/10.1061/(ASCE)1090-0241(2006)132:8(1032)

Olsen R.S. (1997). Cyclic liquefaction based on the cone penetration test. *Proceeding of the NCEER Workshop on Evaluation of Liquefaction Resistance of Soils.* National Centre for Earthquake Engineering, State University of New York at Buffalo, New York, USA,pp. 225–276.

Robertson P.K. & Wride C.E. (1998). Evaluating cyclic liquefaction potential using the cone penetration test. *Journal of the Geotechnical Engineering of Canada* **35**(3): 442–459.
DOI: https://doi.org/10.1139/t98-017

Schneider J.A. & Mayne P.W. (2000). Liquefaction response of soil in Mid-America evaluated by seismic cone tests. *ASCE Geotechnical Special Publication* **97**: 1–16.
DOI: https://doi.org/10.1061/40505(285)1

Seed H.B. & de Alba P. (1986). Use of SPT and CPT tests for evaluating liquefaction resistance of sands. *Proceedings of the Special Conference on Use of in situ Testing in Geotechnical Engineering, Geotechnical Special Publication* **6**: 281–302.

Seed H.B. & Idriss I.M. (1967). Analysis of soil liquefaction: Niigata earthquake. *Journal of the Soil Mechanics and Foundation Division* **93**(3): 83–108.
DOI: https://doi.org/10.1061/JSFEAQ.0000981

Seed H.B. & Idriss I.M. (1971). Simplified procedure for evaluating soil liquefaction potential. *Journal of the Geotechnical Engineering Division* **97**(9): 1249–1273.
DOI: https://doi.org/10.1061/JSFEAQ.0001662

Seed H.B. & Idriss I.M. (1982). Ground motions and soil liquefaction during earthquakes. In : *Earthquake Engineering Research Institute Monograph.* Earthquake Engineering Research Institute, Oakland, California, USA.

Seneviratne H.N., Perera L.R.K., Wijesundara K.K., Dananjaya R.M.S. & de S. Jayawardena U. (2020). Seismicity around Sri Lanka from historical records and its engineering implications. *Engineer* **53**(2): 47–52.
DOI: https://doi.org/10.4038/engineer.v53i2.7412

Shibata T. & Teparaska W. (1988). Evaluation of liquefaction potentials of soils using cone penetration tests. *Soils and Foundations* **28**(2): 49–60.
DOI: https://doi.org/10.3208/sandf1972.28.2_49

Sonmez H. (2003). Modification of the liquefaction potential index and liquefaction susceptibility mapping for a liquefaction-prone area (Inegol, Turkey). *Environmental Geology* **44**: 862–871.
DOI: https://doi.org/10.1007/s00254-003-0831-0

Stark T.D. & Olson S.M. (1995). Liquefaction resistance using CPT and field case histories. *Journal of the Geotechnical Engineering* **121**(12): 856–869.
DOI: https://doi.org/10.1061/(ASCE)0733-9410(1995)121:12(856)

Tokimatsu K. & Asaka A. (1998). Effects of liquefaction-induced ground displacements on pile performance in the 1995 Hyogoken Nambu earthquake. *Soils and Foundations* **2**(Sp): 163–178.
DOI: https://doi.org/10.3208/sandf.38.Special_163

Uduweriya S.B., Wijesundara K.K., Dissanayake P.B.R., Susantha K.A.S. & Seneviratne H.N. (2020). Seismic response of Sri Lanka using PSHA technique. *Engineer* **53**(2): 39–45.
DOI: https://doi.org/10.4038/engineer.v53i2.7411

Ulusay R. & Kuru T. (2004). 1998 Adana-Ceyhan (Turkey) earthquake and a preliminary microzonation based on liquefaction potential for Ceyhan Town. *Journal of the Natural Hazards* **32**: 59–88.
DOI: https://doi.org/10.1023/B:NHAZ.0000026790.71304.32

Weerasinghe D.R., Seneviratne H.N., Kurukulasuriya L.C. & Wijesundara K.K. (2020). Seismic response of Sri Lanka using DSHA technique. *Engineer* **53**(2): 33–37.
DOI: https://doi.org/10.4038/engineer.v53i2.7410

Yasuda S., Harada K., Ishikawa K. & Kanemaru Y. (2012). Characteristics of liquefaction in Tokyo Bay area by the 2011 Great East Japan Earthquake. *Soils and Foundations* **52**(5): 793–810.
DOI: https://doi.org/10.1016/j.sandf.2012.11.004

Youd *et al.* (21 authors) (2001). Liquefaction resistance of soils - Summary report from the 1996 NCEER and 1998 NCEER/NSF workshops on evaluation of liquefaction resistance of soils. *Geotechnical and Geoenvironment Eng*ineering **127**(10): 817–833.
DOI: https://doi.org/10.1061/(ASCE)1090-0241(2001)127:10(817)

Youd T.L. & Perkins D.M. (1978). Mapping liquefaction-induced ground failure potential. *Journal of the Geotechnical Engineering Division* **104**: 443– 446.
DOI: https://doi.org/10.1061/AJGEB6.0000612

Zhang G., Robertson P.K. & Brachman R.W.I. (2004). Estimating liquefaction-induced lateral displacements using the standard penetration test or cone penetration test. *Geotechnical and Geoenvironment Engineering ASCE* **130**(8): 861– 871.
DOI: https://doi.org/10.1061/(ASCE)1090-0241(2004)130:8(861)